

RESEARCH

Open Access



# Comprehensive analysis of pepper (*Capsicum annuum*) RAV genes family and functional identification of *CaRAV1* under chilling stress

Minkun Pei<sup>1,2</sup>, Ping Yang<sup>2</sup>, Jian Li<sup>2,3</sup>, Yan Zhuang Wang<sup>2,4</sup>, Juan Li<sup>2,4</sup>, Hongjun Xu<sup>1\*</sup> and Jie Li<sup>2\*</sup>

## Abstract

**Background** Despite its known significance in plant abiotic stress responses, the role of the RAV gene family in the response of *Capsicum annuum* to chilling stress remains largely unexplored.

**Results** In this study, we identified and characterized six members of the CaRAV gene subfamily in pepper plants through genome-wide analysis. Subsequently, the CaRAV subfamily was classified into four branches based on homology with *Arabidopsis thaliana*, each exhibiting relatively conserved domains within the branch. We discovered that light response elements accounted for the majority of CaRAVs, whereas low-temperature response elements were specific to the NGA gene subfamily. After pepper plants were subjected to chilling stress, qRT-PCR analysis revealed that *CaRAV1*, *CaRAV2* and *CaNGA1* were significantly induced in response to chilling stress, indicating that CaRAVs play a role in the response to chilling stress. Using virus-induced gene silencing (VIGS) vectors, we targeted key members of the CaRAV gene family. Under normal growth conditions, the MDA content and SOD enzyme activity of the silenced plants were slightly greater than those of the control plants, and the REC activity was significantly greater than that of the control plants. The levels of MDA and electrolyte leakage were greater in the silenced plants after they were exposed to chilling stress, and the POD and CAT enzyme activities were significantly lower than those in the control, which was particularly evident under repeated chilling stress. In addition, the relative expression of *CaPOD* and *CaCAT* was greater in V2 plants upon repeated chilling stress, especially *CaCAT* was significantly greater in V2 plants than in the other two silenced plants, with 3.29 and 1.10 increases within 12 and 24 h. These findings suggest that *CaRAV1* and *CaNGA1* positively regulate the response to chilling stress.

**Conclusions** Silencing of key members of the CaRAV gene family results in increased susceptibility to chilling damage and reduced antioxidant enzyme activity in plants, particularly under repeated chilling stress. This study provides valuable information for understanding the classification and putative functions of RAV transcription factors in pepper plants.

**Keywords** RAV gene family, Transcription factor, Chilling stress, VIGS

\*Correspondence:

Hongjun Xu  
xhj@xjau.edu.cn  
Jie Li  
gsau23@126.com

Full list of author information is available at the end of the article



© The Author(s) 2024. **Open Access** This article is licensed under a Creative Commons Attribution-NonCommercial-NoDerivatives 4.0 International License, which permits any non-commercial use, sharing, distribution and reproduction in any medium or format, as long as you give appropriate credit to the original author(s) and the source, provide a link to the Creative Commons licence, and indicate if you modified the licensed material. You do not have permission under this licence to share adapted material derived from this article or parts of it. The images or other third party material in this article are included in the article's Creative Commons licence, unless indicated otherwise in a credit line to the material. If material is not included in the article's Creative Commons licence and your intended use is not permitted by statutory regulation or exceeds the permitted use, you will need to obtain permission directly from the copyright holder. To view a copy of this licence, visit <http://creativecommons.org/licenses/by-nc-nd/4.0/>.

## Background

The B3 transcription factor (TF) significantly influences the ability of plants to respond to stress, growth and development. This domain typically manifests as a DNA–protein binding domain in plants [1]. Several distinct groups of B3 TFs exist, including REM, LAV, RAV and ARF families. Recent research has indicated that there is a fifth member, HSI, which expands the B3 superfamily evolutionary footprint and is particularly evident in cruciferous plants [2]. This expansion has led to the emergence of more complex structures, such as domain repeats and gene tandem repeats. Notably, this situation is unique among ABI3/VP1 (RAV) transcription factors in greater plants [3]. Most B3 superfamily genes feature at least one B3 domain; however, certain RAV gene subfamilies also contain a second domain known as APET–ALA2 (AP2). Akhter et al. classified genes that exhibited double domains and domain replication as members of the RAV subfamily [4]. On the other hand, the RAV subfamily, which is comprised of a single B3 domain, is commonly referred to as the NGA translation factor subfamily. Thirteen RAV family members have been identified thus far in Arabidopsis. Among these, six include an AP2 domain, and seven are members of the NGA subfamily [5]. RAV, a multifunctional transcription factor, has been implicated in the negative regulation of plant growth under various stress conditions, including salt stress and drought, across multiple plant species, such as rice [6], soybean [7], barley [8], cotton [9, 10] and cucumber [11]. Additionally, abscisic acid (ABA), auxin (IAA), and additional stresses regulate RAV expression [12]. Previous studies have employed Arabidopsis RAV1 as a transcription factor for chilling stress [13]. More recent reports have further substantiated this claim. RAV expression in pepper [14], tea [15] and rape [16] plants is upregulated under chilling stress. In addition to its known regulatory effects on ABA and brassinosteroids (BRs) as well as its role in the abiotic stress response, Song et al. reported that the celery RAV negatively regulates zeaxanthin cyclooxygenase (ZEP) and ultimately positively regulates carotenoid synthesis [17]. Although RAV TFs have been studied in various species, the number and functions of pepper RAV TFs are still unclear.

Peppers (*Capsicum annuum* L.) are a pivotal cash crop with a long history of cultivation [18]. Peppers are the second largest vegetable crop globally and span a plant area of 1.4–1.6 million hectares. However, their susceptibility to temperature and light renders them vulnerable to damage under conditions of low temperature and inadequate light exposure. Especially during autumn and spring, low temperatures and low light have a significantly influence both the productivity and quality of peppers [19]. Moreover, growth and development are impeded, and

yields diminish when temperatures drop below 15 °C or light intensity falls below 25  $\mu\text{mol}\cdot\text{m}^{-2}\cdot\text{s}^{-1}$  [20]. Low temperatures not only have a macroscopic impact on plants but also disrupt their intracellular metabolic equilibrium. Upon initial exposure to low temperature, plants experience an accumulation of reactive oxygen species (ROS) within their cells, resulting in the peroxidation of membrane lipids. When the production of reactive oxygen species (ROS) surpasses the ability of the plant to remove them, an imbalance of antioxidants occurs and triggers an oxidative stress response, which in turn can induce DNA damage [21].

Although reports on the RAV transcription factor subfamily exist, detailed information on the specific activities of its members, apart from RAV1, remains limited. A comprehensive characterization of the RAV gene family in pepper plants, especially its response mechanisms to chilling stress, has yet to be performed. This study identified six RAVs within the entire pepper genome and analysed them. Conserved domain evolutionary relationships, gene structure, and *cis*-acting elements in the promoter region were identified. Additionally, virus-induced gene silencing and quantitative real-time PCR (qRT–PCR) were employed to investigate the expression patterns of key genes from the *CaRAV* genes family in response to low temperatures. These results indicate that RAV proteins may play roles in plant responses to chilling stress. Given the potential importance of RAV in plant responses to chilling stress environments, the aim of this study was to examine the impact of the *CaRAV1* and *CaNGAI*, which are characterized by distinct domains, on pepper plants experiencing chilling stress.

## Materials and methods

### Identification of gene family members

The genomic DNA sequences, cDNA sequences, and coding sequences (CDSs) of the *Solanum lycopersicum*, *Capsicum annuum*, and *Arabidopsis thaliana* were obtained from the Ensembl Plants database (<http://plants.ensembl.org/index.html>). The *AtRAVs* gene family database (<https://www.arabidopsis.org/browse/genefamily/index.jsp>) was accessed to obtain 13 protein sequences belonging to the Arabidopsis RAV family. AtRAV proteins were used as query sequences, and the NCBI online software BLASTP was used to search for predicted pepper proteins (<https://blast.ncbi.nlm.nih.gov/Blast.cgi>). The conserved domain of the protein was identified via the second alignment of pepper protein sequences in the InterPro online software (<https://www.ebi.ac.uk/interpro/search/sequence/>). Subsequently, sequences that were in a disarray state were eliminated, resulting in the acquisition of pepper B3 family genes.

### Physicochemical properties of amino acids in the CaRAV subfamily

The amino acid length, relative molecule, relative isoelectric point, amino acid stability, fat solubility index, and average hydrophilic coefficient of the pepper *CaRAVs* were predicted using an online website (<https://web.ExPASy.org/protparam/>). Subsequently, subcellular localization prediction of the gene was performed using online software (<http://www.csbio.sjtu.edu.cn/bioinf/Cell-PLoc-2/>).

### Protein structure prediction for the CaRAV subfamily

Using PSIPRED online software (<http://bioinf.cs.ucl.ac.uk/psipred/>) and SWISS-MODEL (<https://swisssmol.org/>) provided by the protein expert system ExPASy, the secondary structures of proteins encoded by target *CaRAVs* were predicted.

### Analysis of the domains, gene structure and phylogenetic tree

The amino acid sequences of the target *CaRAVs* were compared with those of Clustal 2.1, and the online tool MEME (<https://meme-suite.org/meme/tools/meme>) was used to identify highly conserved motifs. Highly homologous RAV transcription factors from rice and Arabidopsis that matched each target *CaRAV* were acquired from the PlantTFDB transcription factor database (<http://planttfdb.cbi.pku.edu.cn/>). A phylogenetic tree was then constructed using the neighbour-joining (NJ) method in the software MEGA X. The relevant parameter settings were as follows: the bootstrap value was set to 500, the partition deletion was set to 50%, and the genetic distance model was selected as JTT + G for calculation, which is the optimal recommendation. The remaining parameter values were set to their default values.

### Prediction analysis of *cis*-acting elements in the CaRAV promoter

The promoter region (2000 bp upstream of ATG) of the target *RAV* was obtained from NCBI (<https://www.ncbi.nlm.nih.gov/>). The *cis*-acting elements of the promoter region were screened and analysed using PlantCARE. The PlantCARE website (<https://bioinformatics.psb.ugent.be/webtools/plantcare/html/>) was utilized to examine and analyse the *cis*-acting elements found in the promoter region.

### Collinearity analysis of the *CaRAV* gene family

The collinearity analysis was conducted using the MCS-canX software, and the resulting collinearity data were visualized using TBtools, which can be found at the following link: <https://github.com/CJ-Chen/TBtools>.

### Plant materials and chilling stress treatment

The test material used was *Capsicum annuum* “Shenghan 740”. The seedlings were grown in a mixed substrate consisting of peat, perlite, and vermiculite at a ratio of 3:1:1 (v/v). The plants were cultivated at 25 °C with a photoperiod of 12 h and a relative humidity of 75%. When pepper plants reached 5–6 true leaves, the fourth true leaf from top to bottom was selected and veins were removed, 100 mg of each of the silenced plants (pTRV2:*GFP*, pTRV2:*PDS*, pTRV2:*RAV1*, pTRV2:*NGA1*) were stored in liquid nitrogen, and 100 mg of WT was taken as a control sample (Ctl). Then, they were simultaneously placed in a 5 °C thermostat for initial chilling stress treatment (Str0) for 1, 3, 5, 7, 12, 24, 48, and 72 h. In this section, pepper material that was initially chilling stressed for 24 h was recovered at 25 °C for 24 h (Rec), and the recovered material was then subjected to another low temperature to complete the repeated chilling stress (Str1). These treated leaves were promptly frozen in liquid nitrogen for further experiments. Each treatment was replicated at least three times.

### qRT-PCR

Leaf samples (100 mg) were pulverized in liquid nitrogen, and total RNA was isolated using a TRIzol kit (Beijing Tsingke Biotech Co., Ltd.) following the provided instructions. The RNA concentration was measured using a NanoDrop microspectrophotometer (Thermo Fisher Scientific, USA), and its purity was assessed using the A260/280 ratio. The A260/280 ratio was used to determine the purity of the sample. The error-free RNA was diluted to a concentration of 400 ng/μL using distilled water and then stored at -80 °C for subsequent reverse transcription. Complementary DNA (cDNA) was synthesized in the reverse direction using Tsingke RT6 reverse transcriptase following the provided instructions. cDNA was synthesized by designing real-time quantitative primers using Primer-BLAST from the NCBI website. The chimeric fluorescence method was used, with pepper *Actin* serving as an internal reference and SYBR Green I from Tsingke Biotech used as the fluorescent dye. Real-time polymerase chain reaction (PCR) was performed using a Bio-Rad system. The primers used can be found in Supplementary Table 1 online. The relative expression of genes was calculated using the  $2^{-\Delta\Delta C_t}$  method. Three replicates were performed for each sample.

### Vector construction

The ligation primer was designed using CE Design V1.03 software based on the target gene sequence and intended for use with the tobacco rattle virus (TRV) vector. The length of the primer fragment containing the homology

arm of the vector was approximately 40 bp. The process of obtaining RNA has been previously described. However, the acquisition of cDNA differs from that of qRT-PCR because the reverse transcription system utilizes Oligo (dT<sub>17</sub>) instead of Randomer. Rapid 2×Taq Master Mix from the Nanjing Vazyme Biotech Co., Ltd. was used to amplify the target gene fragment. Next, SmaI enzyme digestion was used to release the linear fragment of the TRV vector. The 300 bp purified fragment was connected to TRV using T4 ligase (A 300 bp fragment of the target gene is shown in Supplementary Table 2 online). The monoclonal antibody (Kanamycin) was then incubated with the cells overnight on an inverted plate. Positive clones were identified through electrophoresis after a single colony was shaken at 37 °C for 12 h. To identify false-positive vectors, verifying whether they align with the target sequence during the sequencing process is essential. Following sequencing, the *Escherichia coli* solution containing the homologous arm was subsequently transferred to *Agrobacterium* competent GV3101. The *Agrobacterium* was then cultured on three different antibiotics: kanamycin, gentamicin, and rifampicin. Following agitation of the bacteria in a solitary colony, electrophoresis was subsequently performed to verify the uniformity of the vectors. Ultimately, the silencing vectors pTRV2:RAV1, pTRV2:NGA1, and pTRV2:PDS were generated. Fifty percent glycerin was combined with the bacterial solution at a 1:1 ratio, and the mixture was stored at -80 °C.

#### Silencing efficiency assay for VIGS vectors

A single colony was selected after the vector containing the target fragment was coated with three antibodies on Luria–Bertani (LB) solid media and cultured at 28 °C for two days. 12 h after the initial bacterial suspension was shaken, suitable concentrations of acetosyringone (AS) and 2-morpholinoethanesulfonic acid (MES) were added to the second shaking bacterial suspension. The mixture was then incubated for 12 h and subsequently subjected to centrifugation at 4000 rpm for 15 min at 4 °C. The infection buffer was prepared, and the bacterial solution was resuspended in MaCl<sub>2</sub> buffer solution. The bacterial suspension (OD<sub>600</sub>) was diluted to approximately 0.04 using a buffer solution. A 1:1 ratio of infected liquid pTRV1 was combined with pTRV2:GFP (blank vector with label), pTRV2:PDS (positive albino control), pTRV2:RAV1, and pTRV2:NGA1 to infect the leaves. Virus-infected seedlings were placed in a temperature-controlled room with 75% humidity and 22 °C for 24 h. After this time, the growth conditions were maintained at a temperature of approximately 22 °C, following a standard photoperiod of 12 h of light and 12 h of

darkness. After three days of culture, the fluorescence emitted by GFP, which had been labelled with a green dye, was observed using a 254 nm ultraviolet lamp. After approximately two weeks, the pTRV2:PDS plants were albino and subjected to qRT-PCR analysis to determine their silencing efficiency. Sixty plants with a silencing efficiency above 50% and sixty plants with pTRV2 were chosen for low-temperature treatment.

#### Quantification of the malondialdehyde (MDA) concentration, membrane permeability and antioxidant enzyme activity

The MDA concentration was ascertained using a modified version of the thiobarbituric acid colorimetry method as described by Dhindsa [22]. The relative membrane permeability (REC) was calculated as a percentage according to Yang et al. [23]. The quantification of superoxide dismutase (SOD), catalase (CAT), and peroxidase (POD) activity was conducted using the guaiacol method as described by Jebara et al. [24] and Almeselmani [25]. The relative expression of *CaSOD*, *CaPOD*, and *CaCAT* was quantified using qRT-PCR, and the primers used can be found in Supplementary Table 1 online. SPSS version 19.0 software was used to analyse the significance of differences by one-way ANOVA.

## Results

#### Identification and prediction of the physicochemical properties of CaRAV family genes

BLAST analysis was performed using the Arabidopsis B3 transcription factor family and the complete pepper genome, resulting in the prediction of 12 related pepper CDSs. The software TBtools was utilized to acquire the 12 protein sequences. Subsequently, the structural domains were identified, and the extraneous sequences were eliminated using InterPro. Ultimately, among all the identified proteins, only six were classified as typical pepper RAV proteins, as indicated in Supplementary Table 3. To summarize, a total of six candidate genes were verified as members of the pepper RAV family. Based on the homology of the AtRAVs of CaRAVs, CaRAVs with different structural domains were named CaRAV1, CaRAV2, CaRAV3, CaNGA1, CaNGA2 and CaNGA3 in this study.

According to the results presented in Table 1, all the CaRAVs were found in the nucleus, while CaNGA3 was also present in the cytoplasm. The amino acid length of the CaRAVs ranged from 130 to 480 aa. Specifically, CaRAV2 had the fewest amino acids with a length of 137 aa, while CaRAV3 had the greatest number of amino acids with a length of 477 aa. The molecular weights of the CaRAVs ranged from 14,940 to 52,496 kDa. Among them, CaRAV3 had the highest molecular weight

**Table 1** Analysis of important physicochemical properties of amino acids encoded by CaRAVs

Amino acid	Number of amino acids(aa)	Molecular weight (kDa)	Theoretical (pI)	Instability index	Grand average of hydropathicity	Aliphatic index	Subcellular localization
CaRAV1	244	27,790.89	9.78	26.65	-0.577	75.82	Nucleus
CaRAV2	137	14,940.15	6.58	43.65	-0.472	66.28	Nucleus
CaRAV3	477	52,495.23	6.16	59.1	-0.538	60.27	Nucleus
CaNGA1	176	20,310.77	6.12	37.02	-0.603	71.93	Nucleus
CaNGA2	331	38,699.81	5.93	38.23	-0.679	69.15	Nucleus
CaNGA3	357	40,182.73	8.3	53.62	-0.728	52.91	Cytoplasm/Nucleus

(52,495.23 kDa), while CaRAV1 had the lowest molecular weight (14,940.15 kDa). The isoelectric points of the CaRAVs varied between 5.93 and 9.78, with CaRAV2 having the highest isoelectric point of 9.78 and CaNGA2 having the lowest isoelectric point of 5.93. Furthermore, the stability index (>40) and average total hydrophilicity (<-0.5) suggest that CaRAV1, CaRAV3, and CaNGA3 are both unstable and hydrophilic. On the other hand, CaRAV2, CaNGA1, and CaNGA2 are both stable and hydrophilic.

**Distribution of CaRAVs on chromosomes**

Using TBtools software in conjunction with pepper genome annotation files, the location and distribution

of CaRAVs were mapped on chromosomes. The graph (Fig. 1) shows that among the 12 chromosomes of peppers (see Supplementary Table 4 online), CaRAVs were exclusively found on Chr1, Chr10, Chr11 and Chr12. Chr1 and Chr11 each had two members, while the other two chromosomes had only one RAV. Moreover, all members of this gene family were located at the ends of chromosomes, and no RAV was present in the middle region of any chromosome. A linkage region comprised of the genes CaRAV1 and CaRAV2 was established at the beginning of Chr11. The two genes were surrounded by continuous bases extending 100 bp upstream and downstream based on their location and length.

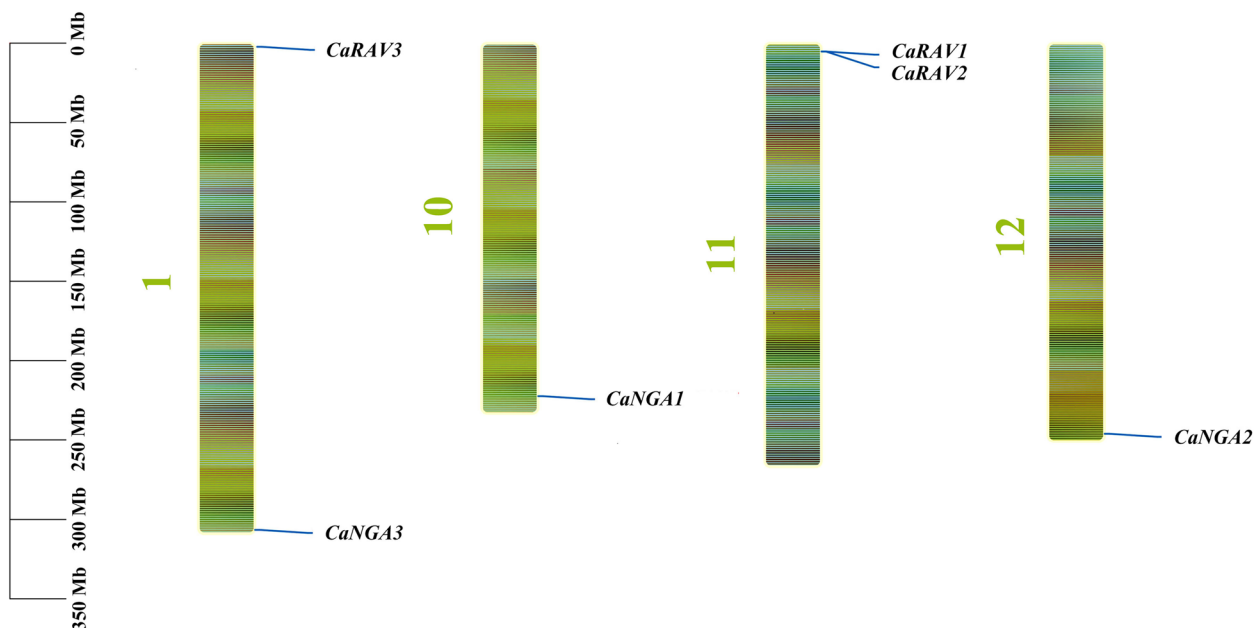


**Fig. 1** Diagram illustrating the arrangement of pepper RAVs on the chromosomes. The chromosomes of the pepper plants are represented by vertical bars. The chromosome number is displayed adjacent to each chromosome. The vertical axis on the left side of the diagram represents the length of the chromosomes



**Table 2** Secondary structure analysis of the CaRAVs protein

Protein	β-Strand amount	β-Strand	Helix amount	Helix	Coil amount	Coil
CaRAV1	59	24.18%	35	14.34%	150	61.48%
CaRAV2	17	12.41%	16	11.68%	104	75.91%
CaRAV3	56	11.74%	46	9.64%	375	78.62%
CaNGA1	51	28.98%	22	12.50%	103	58.52%
CaNGA2	55	16.62%	111	33.53%	165	49.85%
CaNGA3	65	18.21%	20	5.60%	272	76.19%

**CaRAV protein structure correlation**

PSIPRED software was used to predict the secondary structure of the proteins. The results (Table 2) revealed that the CaRAV proteins consisted of three components: a β corner, an extended main chain, and an irregular curl (see Supplementary Fig. 1 online). However, the relative sizes of each structure varied. Irregular curling accounted for 49.85% to 78.62% of the total proportion. The β rotation angle and extended main chain components had relatively low percentages, ranging from 11.74% to 28.98% and 5.60% to 33.53%, respectively. These findings indicated that the primary secondary structure of CaRAVs is an irregular curl.



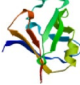



SWISS-MODEL was used to predict the tertiary structure of the CaRAV proteins (Table 3). The alignment rate between all members of the CaRAVs and templates exceeded 70%, and the root mean square deviation

(RMSD) was less than 2.5 Å. These findings suggest that the homology modelling outcomes are reasonably dependable [26]. CaNGA1, CaNGA2 and CaNGA3 matched protein templates containing the B3 structural domain, whereas CaRAV1, CaRAV2 and CaRAV3 matched protein templates containing both the B3 and AP2 structural domains.

**Phylogenetic tree of CaRAVs, SIRAVs and AtRAVs**

The amino acid sequences of CaRAVs were searched for homology via BLAST in PlantTFDB. RAV proteins in Arabidopsis and tomato that were found to be highly homologous to CaRAVs (top 10 in terms of score) were screened, repetitive sequences were eliminated, and a phylogenetic tree was constructed using 9 SIRAVs and 13 AtRAVs in conjunction with the 6 CaRAVs (Fig. 2). The findings indicated that all individuals from the three species were classified into four

**Table 3** Analysis of the tertiary structure of the CaRAVs protein

Medel	Protein	Seq Identity	RMSD	Oligo-state	Ligands	Description
	CaRAV1	100.00	N Å	monomer	None	AP2/ERF and B3 transcription
	CaRAV2	84.13	1.05 Å	monomer	None	AP2/ERF and B3 transcription
	CaRAV3	71.82	1.80 Å	monomer	None	AP2/ERF and B3 transcription
	CaNGA1	74.27	1.65 Å	monomer	None	TF-B3 domain-containing protein
	CaNGA2	100.00	N Å	monomer	None	TF-B3 domain-containing protein
	CaNGA3	100.00	N Å	monomer	None	TF-B3 domain-containing protein

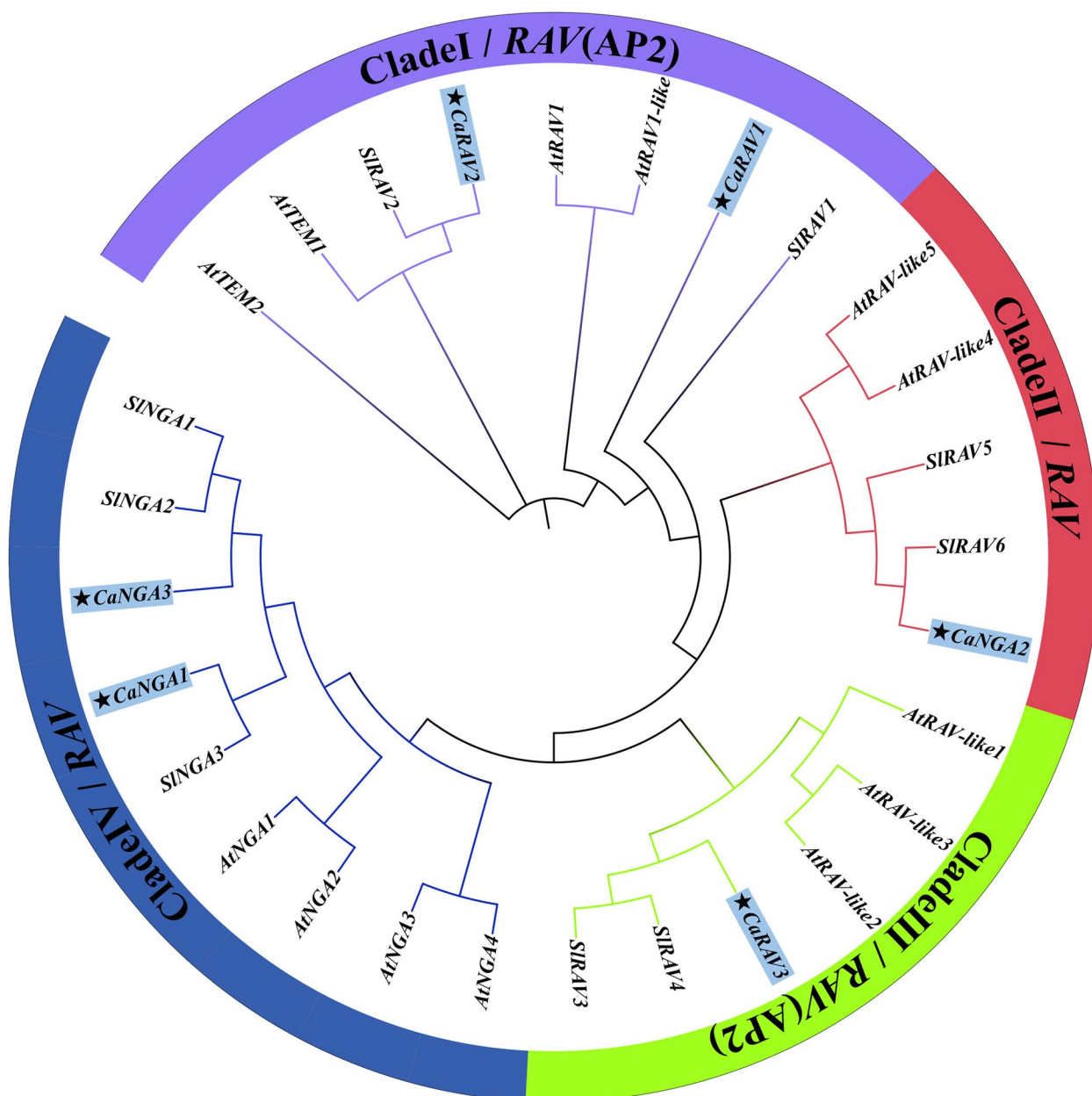


**Fig. 2** Phylogenetic tree without a root, illustrating the connections between the RAV of Arabidopsis, tomato, and pepper. The organisms are categorized into four clades based on their homologous evolutionary relationships. Clades I, II, III, and IV are represented by lilac, carnation, olive-green, and small branch lines, respectively. The RAV obtained from pepper is designated with an asterisk prefix

distinct clusters (I–IV), with minimal variation in the population amount across the four groups. A comparison of phylogenetic trees revealed that SIRAVs and CaRAVs are more homologous than are AtRAVs.

**Phylogenetic tree, gene structure, and domains of AtRAVs, SIRAVs and CaRAVs**

Figure 3 shows the Arabidopsis and tomato RAV gene families in the tree, along with the domains and

conserved sequences of the RAV gene family. Additionally, we included peppers in the analysis. We utilized the MEME online tool to analyse the amino acid sequences of the CaRAVs. From this analysis, we identified 10 conserved motifs based on their *P* values (see Supplementary Table 5 online). The findings indicated variations in the location and abundance of each motif within the amino acid sequence of CaRAVs. Two motifs, motif 1 (LLNFEDENGKVVWRFYSYWNSSQSYV-

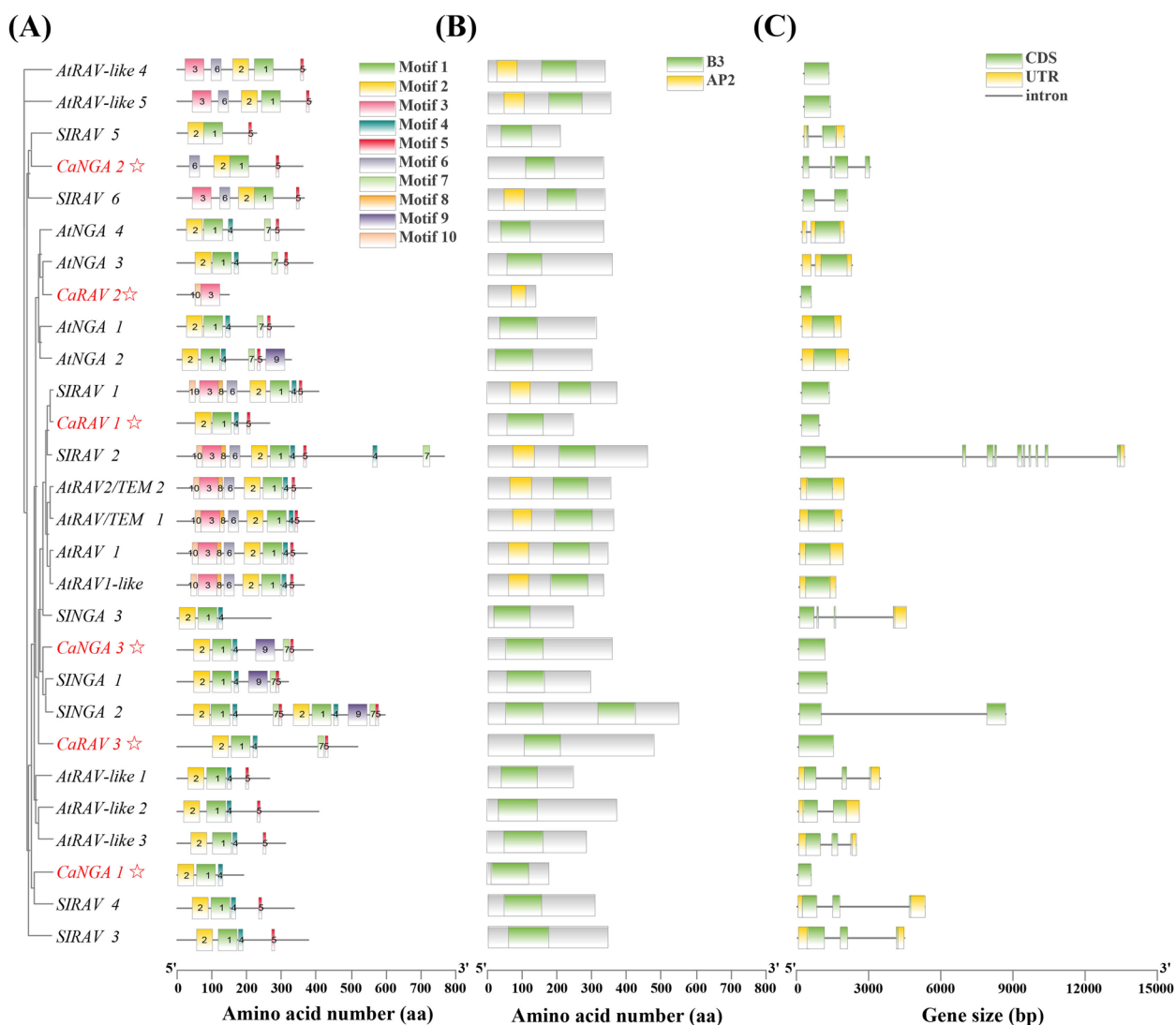


**Fig. 3** Conserved motif, structural domain, and gene structure analysis of AtRAVs, SIRAVs, and CaRAVs gene families. **A** The ten conserved motifs are represented by rectangles of different colors. **B** The domains are shown in three colored rectangles green for B3, yellow for AP2, and gray for non-domain areas. **C** Exons and introns are replaced by green matrices and gray lines, respectively, and can be judged by the number of corresponding colors and rectangles. The black lines indicate relative lengths. The RAV from pepper is labeled with an asterisk suffix

LTKGWSRFVKEKKLDAGDVVSFQR) and motif 2 (ALIEREHLFEKVVTSPDVGKLNRLVIPKQHAEKYFPLDSSN), are found to be highly conserved across various CaRAV sequences. Therefore, motif 1 and motif 2 comprise the conserved region of CaRAV transcription factors. CaRAV2 lacks motif 1 and motif 2, but it exhibits greater similarity to the conserved region of AtRAVs. Additionally, CaRAV2 is highly homologous to CaRAV2 in Arabidopsis (Fig. 3A). However, the cause of this outcome remains uncertain, and it is possible that CaRAVs have undergone a distinct evolutionary

process. CaRAV2 has been determined to have a close relationship with the evolution of Arabidopsis, potentially due to the gene linkage previously observed on the chromosome.

The domain visualization shows that the three species possess only two domains each, namely, the B3 and AP2 domains. Only domains within a 500 bp range are shown in Fig. 3B. The exon–intron structure depicted in Fig. 3C indicates that *CaRAVs* lack introns, with five members consisting of a single exon. In contrast, CaNGA2 contains multiple exons and introns.



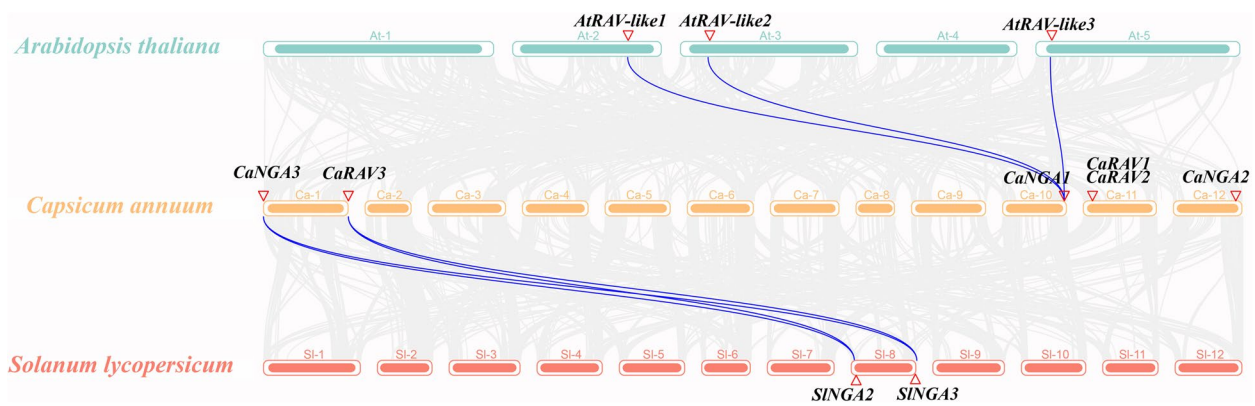


**Fig. 4** Homology analysis of the RAV between pepper and the representative plants Arabidopsis and tomato. The colored circular rectangles denote the chromosomes of the three plants. The grey curves indicate collinear blocks within the genomes, and the blue curves represent collinear gene pairs. The red triangle represents the location of the RAV

**Collinearity of the three species**

To elucidate the evolutionary relationship of the RAVs across various plants, we used the genomes of Arabidopsis, tomato, and pepper plants for collinearity analysis via MCScanX software (Fig. 4). Three pairs of homologous genes were identified in Arabidopsis and pepper (*CaNGA1/AtRAV-like1*, *CaNGA1/AtRAV-like2*, and *CaNGA1/AtRAV-like3*), while two pairs of homologous genes were identified in tomato and pepper (*CaNGA3/SINGA2* and *CaNGA2/SIRAV3*).

**Cis-acting elements in CaRAV gene family promoters**

To determine the biological function of the CaRAVs, an analysis of *cis*-acting elements was conducted on the 2 kb promoter region located upstream of the initiation codon of the CaRAVs. This analysis was performed using the Plant-CARE database. In the CaRAV promoter, we discovered 12 regulatory elements that are

conserved and have a significant impact on the plant stress response (see Supplementary Table 6 online) and growth regulation (Fig. 5A). The promoter region of the CaRAV family contains photoresponsive, MeJA-responsive, and anaerobic-inducing elements. In terms of quantity, light responsive elements are the most abundant. However, low-temperature responsive elements are present only in the CaNGA subfamily. The amount of *cis*-acting elements in CaRAV members also varied to some extent, with CaNGA1 having a maximum of 24 components and CaRAV2 having a minimum of 16 components (Fig. 5B).

**Expression pattern of CaRAVs under chilling stress conditions**

To assess the response of the CaRAVs to natural low temperatures and determine the extent of CaRAV involvement in chilling stress, we conducted qRT-PCR

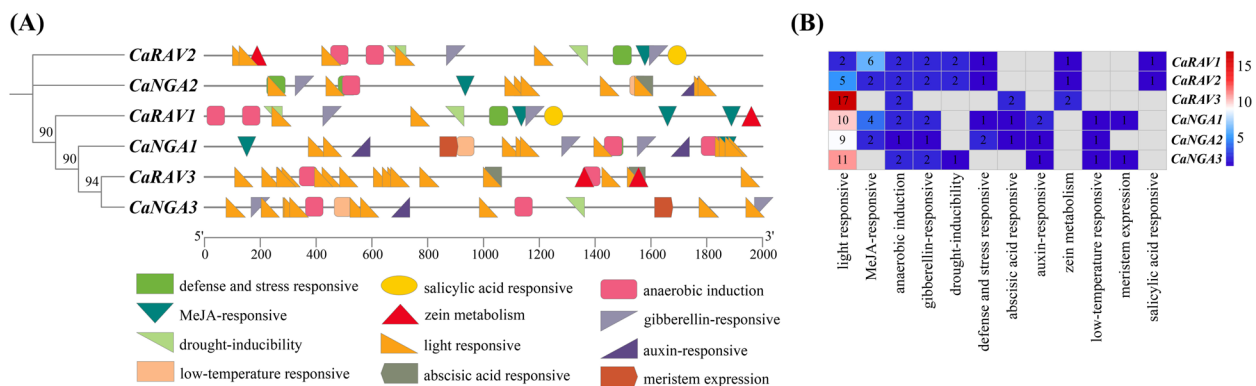


**Fig. 5** Prediction of *cis*-elements in RAV promoters, which are conserved regulatory elements associated with plant hormone response, stress response, and growth regulation. **A** Distribution of the 12 main *cis*-elements in CaRAVs, with different colored shapes indicating the positions of the different elements in the promoter. **B** Clustering heatmap of the number of promoter *cis*-elements. Black numbers are numbers, red means ten or more, and grey means zero

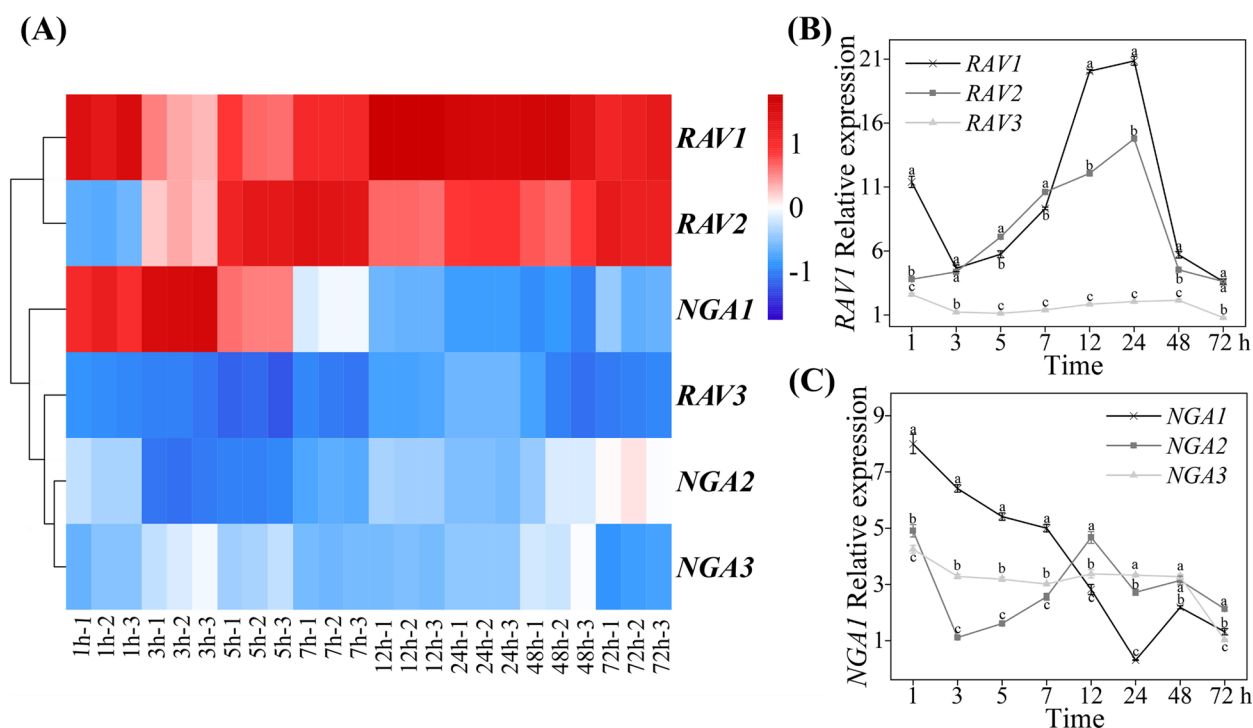


**Fig. 6** The expression profiles of the *CaRAVs* gene subfamily were analysed after the plants were subjected to three days of chilling stress. **A** The expression amount is converted to a 2-based log function and then normalized by column by the row using the normalization method. The color scale to the right of the heatmap indicates the relative expression level, with an elevated expression level shown by the color gradient ranging from dodger blue to red. **B** Relative expression measurements of *CaRAVs*. **C** Relative expression measurements of *CaNGAs*. The relative expression of the initial 0 h is 1. Data shown are means ± SD (n = 3). Different lowercase letters in the table indicate significant differences (p < 0.05, one-way ANOVA)

analysis of the *CaRAVs* after pepper plants were subjected to 3 days of treatment at 5 °C. The relative expression levels of the *CaRAVs* were calculated using pepper *Actin* as an internal reference. The relative expression levels were visualized using a cluster thermograph (Fig. 6). The results demonstrated that the relative expression levels of all examined genes increased following exposure to chilling stress. During periods of chilling stress, the expression of *CaRAVs* is typically elevated at 12 h and 24 h after stress. Among the *CaRAVs*, *CaRAV1*, *CaRAV2*, and *CaNGAI* showed the most significant expression changes. The relative expression of *CaRAV1* increased 20.06-fold and *CaRAV2* 14.77 at 24 h of initial chilling stress compared to 0 h, while *CaNGAI* was able to respond rapidly to the initial stage of low temperature stress, increasing 7.99 at 1 h.

#### Response of *CaRAV1* and *CaNGAI* under repeated chilling stress

Based on qRT-PCR heatmap data, we selected two genes from the *CaRAV* gene family that exhibited the greatest response to chilling stress. These genes are *CaRAV1*, which possesses AP2 and B3 domains, and

*CaNGAI*, which possesses a B3 domain. Low temperatures in nature may occur repeatedly for a period of time. Since there was little change in the relative expression of *CaRAVs* after 24 h of initial stress, the upper limit of the two stresses was set at 24 h (for the chilling response of the wild-type pepper plants, see Supplementary Fig. 2 online). The results showed that the expression of *CaRAV1* and *CaNGAI* was upregulated after 24 h of chilling stress in the Str0 group (Fig. 7). After one day of recovery (Rec), *NGAI* recovered to near its original level, while the level of *RAV1* was significantly greater than that of the control (Ctl). When plants were again subjected to chilling stress (Str1 group), *RAV1* exhibited increased accumulation at 1, 3, 12, and 24 h, and *NGAI* exhibited increased accumulation at 1, 3, 5, and 24 h.

#### Assessment of the effectiveness of silencing *CaRAV1* and *CaNGAI*

To study the role of various domains in the *CaRAV* gene family under chilling stress, we created virus-induced silencing vectors (pTRV2:GFP, pTRV2:*PDS*, pTRV2:*RAV1*, and pTRV2:*NGAI*) using tobacco crisp virus (TRV). All of the electrophoretic bands that were

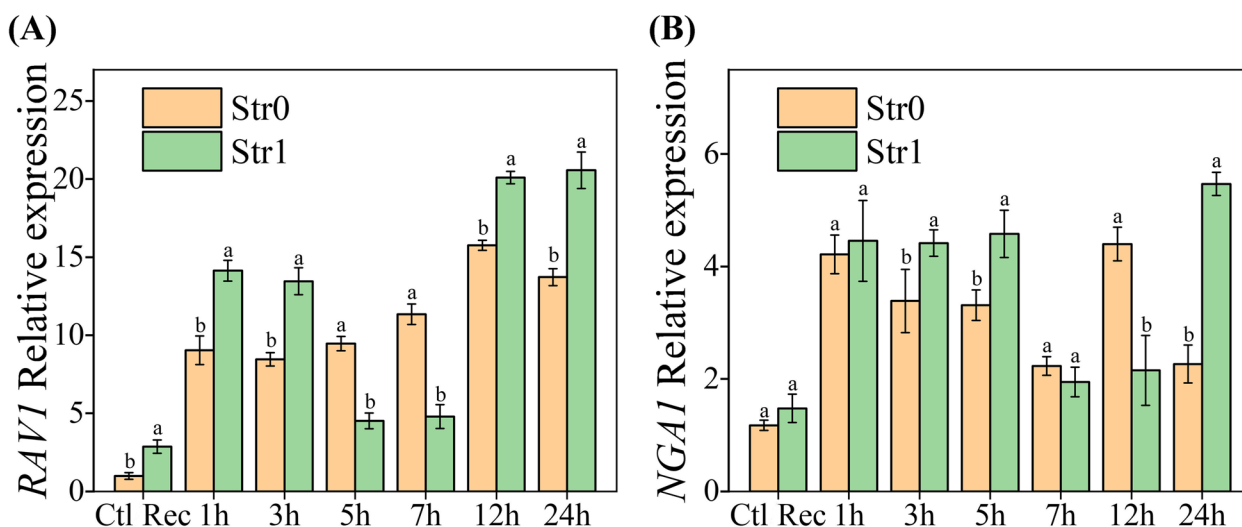


**Fig. 7** Chilling stress induces the expression of *CaRAV1* and *CaNGA1*. The experiment consisted of four treatments: the control group (Ctl); the direct stress group (Str0), which was subjected to chilling stress at 5 °C for 24 h; the recovery group (Rec), which experienced chilling stress for 24 h at 25 °C followed by 1 day of recovery; and the restress group (Str1) which underwent an additional 24 h of chilling stress after the recovery period. Where the yellow rectangle represents Str0 and the green rectangle represents Str1, the 0 h of initial chilling stress (Str0) is indicated by the control group Ctl, and the 0 h of repeated chilling stress (Str1) is indicated by the recovery group Rec. **A** The relative expression of *CaRAV1* was measured in the four treatment groups. **B** The relative expression of *CaNGA1*. The experiments were replicated three times. The provided data represent the mean values of three repeated measurements, with the standard deviation (SD) indicated by the error bars. Data shown are means  $\pm$  SD ( $n=3$ ). Different lowercase letters in the table indicate significant differences ( $p < 0.05$ , one-way ANOVA)

transferred into *Agrobacterium* GV3101 showed positive results when analysed using a gel imaging system, and the length of the target gene fragment was determined to be 300 base pairs (Fig. 8A, C). Plants were infected with *Agrobacterium* vectors when both cotyledons were expanded. After a period of 3–7 days, the presence of green fluorescence, marked by the GFP tag, was detected using a 254 nm ultraviolet lamp. The study revealed that the plants with silenced genes were effectively infected during the initial phase (see Supplementary Fig. 3 online). The silencing efficiency of pTRV2:*PDS* was confirmed by RT-PCR and qRT-PCR after the albino phenotype appeared two weeks later. The findings indicated that the two vectors exhibited substantial suppression of expression in comparison to pTRV2:GFP and the control (Ctl), with a silencing efficiency exceeding 50% (Fig. 8B, D). Once the plants reached the stage of having six true leaves, the GFP label of the silenced plants ceased to exhibit green fluorescence (see Supplementary Fig. 4 online).

**MDA content and relative membrane permeability of the silenced peppers**

The reactions of *CaRAV1* and *CaNGA1* to chilling stress were assessed. With the onset of chilling stress, both silenced plants showed more severe wilting compared to the blank vector V2 plants (see Supplementary

Fig. 6 online). We analysed the indices associated with cell membrane damage (Fig. 9), including the levels of MDA (Fig. 9A) and REC (Fig. 9B), which exhibited a consistent upwards trend with chilling stress. The MDA (malondialdehyde) and REC (relative electrical conductivity) levels in the *RAV1*-silenced plants were generally greater than those in the *NGA1*-silenced plants. In all treatments, plants subjected to low temperature experienced a moderate increase in cell membrane permeability and MDA levels, but their ability to return to the original range was limited. The MDA content was significantly greater in *RAV1*-silenced plants at 12 h after Str0 or Str1 injury than after blank vector (V2) injury, whereas the difference in the MDA content among the three groups of silenced plants at 24 h after Str0 or Str1 injury was not significant. In addition, the RECs exhibited a relatively stable trend in the four treatment groups, and the RECs of the two silenced plants were significantly greater than those of the V2 plants.

**Antioxidant enzyme activity of the silenced peppers**

Low-temperature treatment resulted in an increase in the activity of antioxidant enzymes. However, antioxidant enzyme activities were significantly lower in the silenced plants than in the pTRV2 plants (Fig. 10). After a single day of recovery from the initial chilling stress, the antioxidant enzyme activities of the *RAV1*-silenced plants

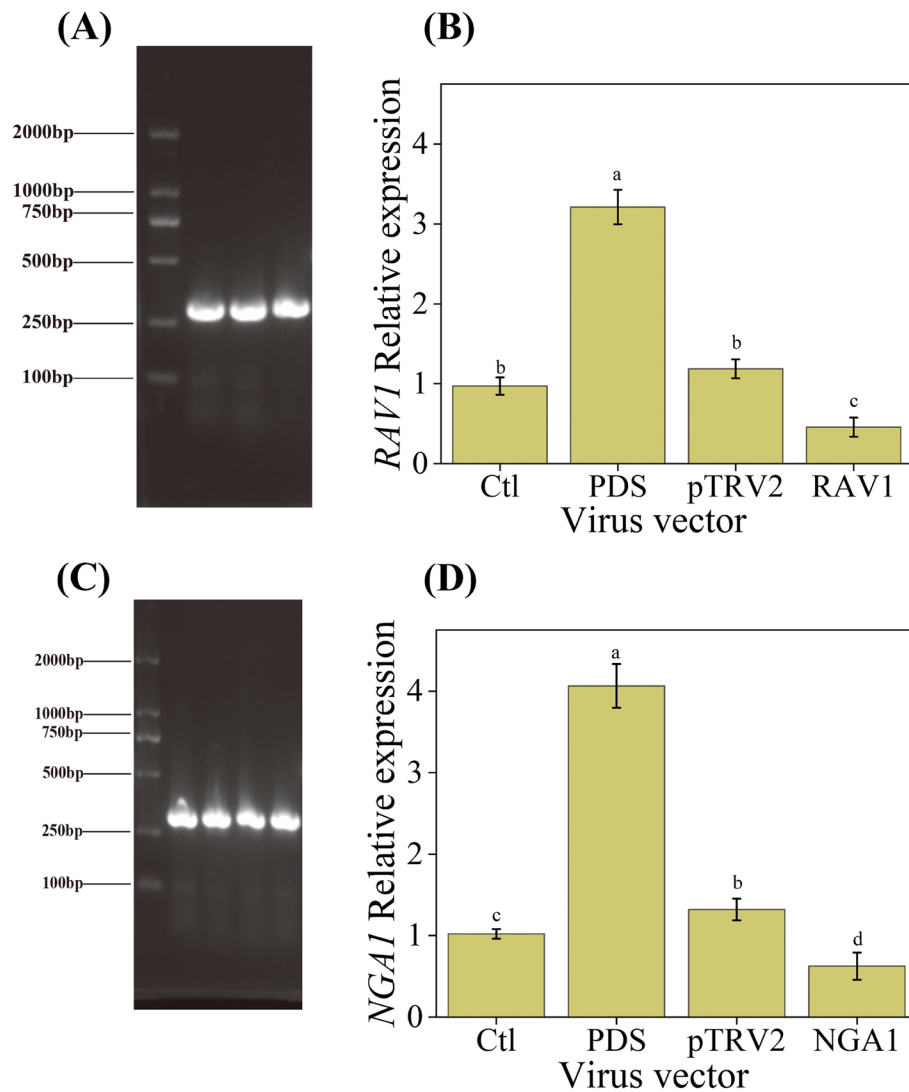


**Fig. 8** Semi-quantitative reverse transcription polymerase chain reaction (RT-PCR) and quantitative reverse transcription polymerase chain reaction (qRT-PCR) were performed to analyse the expression levels of *CaRAV1* and *CaRAV2* in pepper plants subjected to virus-induced gene silencing, full uncropped Gels are shown as Supplementary Fig. 5 online. **A** Maker (2000 bp) is shown on the left side of the Figure. The white band on the right side of Maker, a positive control, is between 250 and 500 bp. It can be inferred that *CaRAV1* contains three groups of repetitions of approximately 300 bp. **B** Horizontal coordinates are four different groups of gene-silenced plants: WT blank control (Ctl), positive control (pTRV2:PDS), blank vector (pTRV2:GFP) and pTRV2:*RAV1*-silenced plants. The vertical coordinate is the relative expression of *CaRAV1*. **C** Semi-quantitative electrophoresis (EP) of *CaNGA1*, which was repeated four times, revealed that the band position was approximately 300 bp. **D** Relative expression of *CaNGA1* in four different groups of gene-silenced plants. One-way ANOVA demonstrated that there was significant difference ( $p < 0.05$ ) between the transgenic lines and WT (Ctl). Different lowercase letters in the table indicate significant differences

were restored to their initial levels; in the *NGA1*-silenced plants, only the CAT enzyme activity was restored to its initial level, and both the SOD and POD activities were significantly reduced. When subjected to chilling stress again, the antioxidant enzyme activities were significantly greater in the V2 plants. The *RAV1*-silenced plants showed a similar trend in SOD and POD enzyme activities over a 12 h period, but the increases in both stresses were smaller than those in the V2 plants. In contrast

to the 12 h of repetitive chilling stress (Str0), SOD and CAT enzyme activities in *NGA1*-silenced plants did not increase, and these enzymes even tended to decrease. In addition, by the relative expression of genes related to antioxidant enzymes, blank vector V2 plants were able to elevate *CaSOD*, *CaPOD*, and *CaCAT* by a factor of 2.29, 1.20, and 1.30, respectively, and were significantly greater than *RAV1*-silenced and *NGA1*-silenced plants after 12 h from the onset of chilling stress. At 12 and

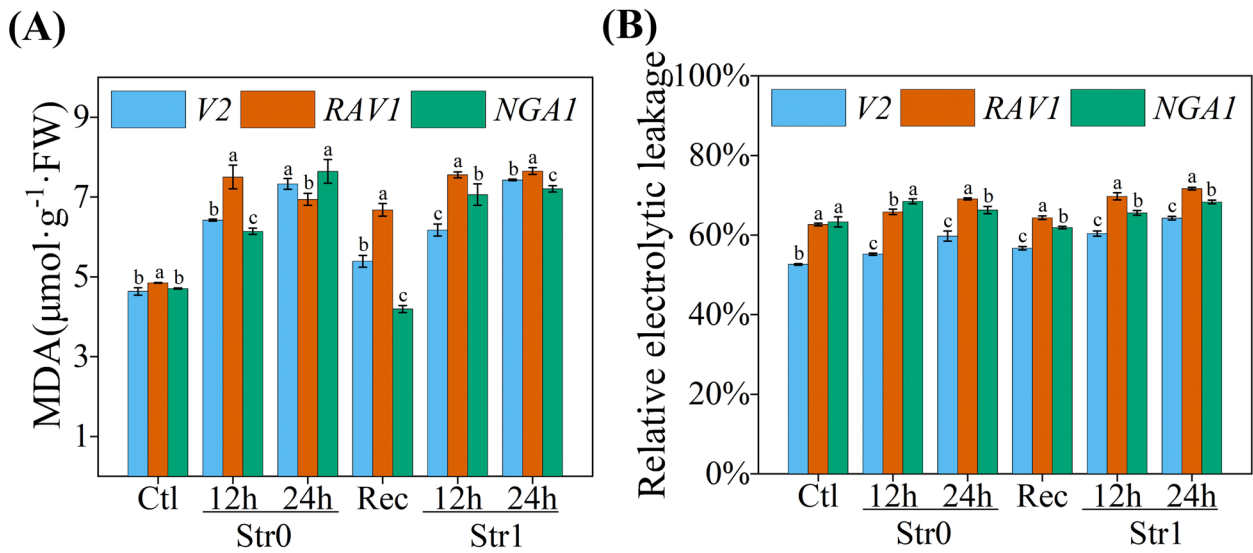


**Fig. 9** Investigate the changes of MDA content and REC in pepper leaves under four different chilling stress treatments. Since the changes in the relative expression of *RAV1* and *NGAI* were more pronounced at 12 and 24 h, only the differences between Str0 and Str1 at 12 and 24 h were examined. The experiment consisted of four treatments: the control group (Ctl); the direct stress group (Str0), which was subjected to chilling stress at 5 °C for 24 h; the recovery group (Rec), which experienced chilling stress for 24 h at 25 °C followed by 1 day of recovery; and the restress group (Str1) which underwent an additional 24 h of chilling stress after the recovery period. **A** MDA content. **B** REC change trend. The presence of distinct letters above or below the error bars indicates significant differences at a significance level of  $p < 0.05$  (one-way ANOVA)

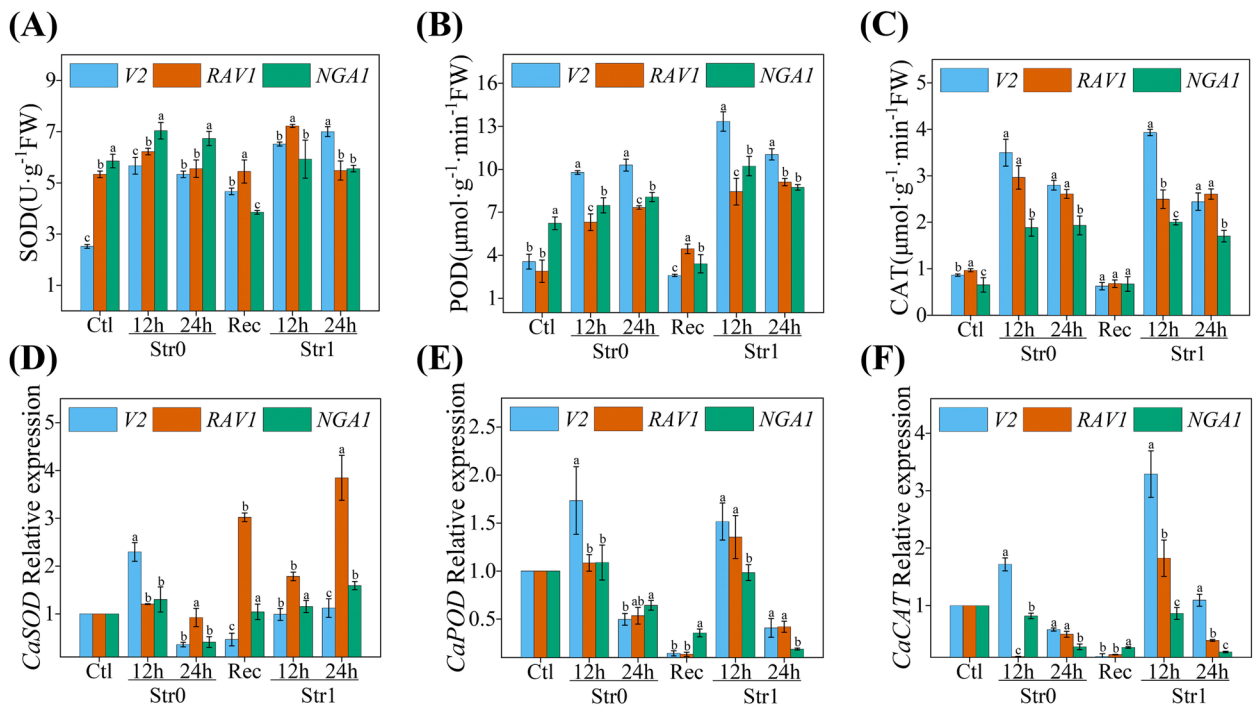


**Fig. 10** Investigation of the changes in SOD, POD and CAT enzyme activities and relative gene expression of *CaSOD*, *CaPOD*, and *CaCAT* in pepper gene silenced plants under four different chilling stress treatments. The experiment consisted of four treatments: the control group (Ctl); the direct stress group (Str0), which was subjected to chilling stress at 5 °C for 24 h; the recovery group (Rec), which experienced chilling stress for 24 h at 25 °C followed by 1 day of recovery; and the restress group (Str1) which underwent an additional 24 h of chilling stress after the recovery period. **A** SOD enzyme activities. **B** POD enzyme activities. **C** CAT enzyme activities. **D** *CaSOD* relative expression. **E** *CaPOD* relative expression. **F** *CaCAT* relative expression. The presence of distinct letters above or below the error bars indicates significant differences at a significance level of  $p < 0.05$  (one-way ANOVA)



24 h of repeated chilling stress (Str1), the relative expression of *CaSOD* in *RAVI*-silenced plants was significantly greater than that in the other two plants, elevated by 1.78 and 3.85, respectively. The relative expression of *CaPOD* and *CaCAT* was greater in V2 plants, and especially the expression of *CaCAT* was significantly greater in V2 plants than in the other two silenced plants, multiplicative increase of 3.29 and 1.10 at 12 and 24 h (Str1).

## Discussion

RAV, one of the subfamilies of the B3 transcription factor superfamily, has been demonstrated to have a significant impact on the physiology and biology of plants. The RAV subfamily is involved in plant growth, development, and responses to abiotic stress. Peppers are a significant horticultural crop in the global economy, and their demand is steadily rising each year [27]. Currently, pepper production often experiences economic and yield losses due to chilling stress. Despite significant advancements in chilling resistance, there is a scarcity of information regarding the response of pepper plants to chilling stress and CaRAVs [28].

This study revealed six members of the RAV gene subfamily in the entire pepper genome. These members include three members with the complete B3 domain, namely, *CaNGA1*, *CaNGA2*, and *CaNGA3*, and two members of them with both the B3 and AP2 domains, namely, *CaRAV1*, and *CaRAV2*. Through chromosome mapping, we determined that the RAV gene family members in peppers exhibit a limited distribution, are distributed at both ends of the chromosome, and are closely related genes. Linkage regions were formed at the top of Chr11, comprising two genes, *CaRAV1* and *CaRAV2*. The 100 bp regions upstream and downstream of these two genes were considered continuous bases. This positional relationship may be associated with the evolutionary development of the RAV gene family and could also impact the regulatory function of *RAV*. Tandem replication is a frequently observed phenomenon in the evolution of plant genomes, particularly in *Solanaceae* plants [29, 30]. These repetitive sequences, known as tandem repeats, have a significant impact on the ability of plants to adapt to environmental changes [31]. In the present study, the relative expression of these two interlocking genes (*CaRAV1* and *CaRAV2*) increased in response to chilling stress.

Compared with those of other members of the CaRAV gene family, the closely associated genes *CaRAV1* and *CaRAV2* exhibited greater and more rapid increases in gene expression. Previous research demonstrated that genes replicated in tandem are more likely to be involved in abiotic stress responses in *Arabidopsis* [32, 33]. Furthermore, based on protein secondary structure

analysis and modelling of homologous proteins, the primary secondary structure of CaRAVs is an irregular curl. The extended backbone and  $\beta$  angle may serve a supplementary and modifying function, thereby aiding in the formation of complex protein conformations at a later stage and performing specific functions. The structural homology of these proteins indicates functional similarity. The 28 members of the three species were classified into four branches based on their gene structure and conserved motifs. This classification was used to construct a phylogenetic tree, which represents the homologous relationships among CaRAVs, AtRAVs, and SIRAVs. The findings indicated that the similarity between pepper and tomato was greater. Furthermore, based on the collinearity analysis of *Arabidopsis*, tomato, and pepper, we discovered that *CaNGA1* exhibited collinearity with three AtRAV members. This finding suggested that these genes likely have comparable functions and contributed significantly to the evolutionary dynamics of RAV gene families in pepper and *Arabidopsis*. Notably, *CaRAV1*, *CaRAV2*, and *CaNGA2* in tomato and *Arabidopsis* do not share a collinear relationship with the other two species, suggesting that these genes may be exclusive to the evolution of peppers. In addition to their role in gene expression regulation, introns also play a role in gene evolution [34]. According to exon–intron analysis, *CaNGA2* exhibited multiple introns, whereas other members lacked introns. Furthermore, among the 13 members in *Arabidopsis*, only 5 possess introns. The origin of intron-free genes and whether they lost introns during evolution or were absent from the beginning of development remain unclear. Studies in *Arabidopsis* have demonstrated that intron-free genes can be significantly activated in response to stress. Additionally, research in rice and *Arabidopsis* has shown that intron-free genes can play a crucial role in adapting to salt stress and drought [35].

Exposure to chilling stress can disrupt the equilibrium of reactive oxygen species in plant cells, resulting in the accumulation of reactive oxygen species and subsequent membrane lipid peroxidation. During this process, plants initiate a highly efficient detoxification system and synchronize the activities of antioxidant enzymes and non-enzymatic substances. Currently, widely recognized antioxidant enzymes include SOD, CAT, POD, and ascorbic acid POD (APX). The accumulation of these enzymes can safeguard plants against harm caused by low temperature [36, 37]. In pepper production, various antistressors are commonly employed to mitigate abiotic stresses [38–41]. Additionally, chilling acclimation is utilized to enhance pepper tolerance to low temperatures [42]. This phenomenon, also known as “stress memory” [43], represents the plasticity mechanism of plants in response to production conditions. Within this study, two genes with

different structural domains, *CaRAVI* and *CaNGAI*, were found to be relatively sensitive to chilling stress. The plants exhibited a recovery period of one day following exposure to low temperatures for one day. The relative expression levels of *CaRAVI* and *CaNGAI* also returned to their original baseline levels with recovery. Under repetitive chilling stress, these genes in plants responded more quickly, thereby increasing their relative expression, which is consistent with the typical epigenetic alterations induced by chilling stress in plants. Interestingly, *CaNGAI*, which showed a similar trend, exhibited some quantitative differences (Figs. 6 and 7) at the beginning of chilling stress (at 1 h). In Fig. 7 the relative expression of *CaNGAI* was elevated by 57.12% in the initial stress (Str0) compared with Fig. 6, but the overall trend was close to the same in both treatments with time. The reason for this result may be that there are some differences in the different batches of plant leaf materials in response to chilling stress. In addition, the reason for such a result is not clear, but in the subsequent cloning of *NGAI* target gene fragments, we found that *NGAI* was enriched in roots, whereas fragments could not be cloned in leaves, which may also explain the sampling location's influence on the content of both. According to qRT-PCR validation of the virus-induced gene-silenced plants, *CaRAVI* exhibited a greater relative expression level subsequent to albinism in the pTRV2:*PDS*-positive plants. The cause of this phenomenon remains uncertain, but may possibly be due to the suppression of octahydro lycopene dehydrogenase (*PDS*) activity, which leads to the inhibition of carotenoid production. As previously stated, *RAV* acts as a suppressor of zeaxanthin cyclooxygenase [44], and *RAVI* and *NGAI* may have significant functions in carotenoid synthesis following *PDS* silencing.

MDA is a significant outcome of membrane peroxidation in plants, while the REC represents the extent of electrolyte leakage in cells. These indicators are crucial for assessing the level of damage to the cell membrane [45, 46]. Typically, these changes are positively correlated with the timing of abiotic stresses, which aligns with the pattern of silenced plant expression observed during a single day of low temperature in this study [47, 48]. When virus-induced gene-silenced plants were subjected to chilling stress for 12 h, the MDA content of the *RAVI*-silenced plants was significantly greater than those of the pTRV2:*NGAI* and V2 plants, and the MDA level and cell membrane permeability of the *RAVI*-silenced plants had difficulty recovering to the initial level of the Ctl. The results of the conductivity assay indicated that the cell membrane damage of the pTRV2:*RAVI* and pTRV2:*NGAI* silenced plants was greater than that of the V2 plants. Furthermore, plants exhibit physiological and biochemical reactions involving cell membrane

systems and protective enzyme systems. SOD, POD, and CAT are crucial enzymes with protective functions in plants. Antioxidants prevent cell membrane damage by specifically targeting reactive oxygen species and nitrogen as well as lipid peroxidation products and transcription factors that control the expression of genes related to antioxidant response elements [49]. The antioxidant enzyme activities of pepper plants were notably greater at 5 °C for 12 and 24 h than at 25 °C for 0 h. These findings align with the results reported by Nai et al. [50]. In plants subjected to gene silencing, SOD and CAT did not show a significant increase in enzyme activity under repeated stress, while POD enzyme activity significantly increased. Moreover, the POD and CAT enzyme activities of the silenced pepper plants were significantly lower than those of the pTRV2 plants in response to chilling stress. *RAVs* may also be involved in the response of pepper plants to chilling stress and increase the tolerance of plants to chilling stress. Repeatedly chilling stressed plants do not produce more severe wilting, in terms of the appearance of plants subjected to low-temperature stress. These findings provide a basis for future investigations into the roles of *RAV* transcription factors in the response of pepper plants to chilling stress. The potential physiological responses identified in this study could be utilized in future molecular studies on enhancing chilling resistance in pepper plants.

## Conclusions

In summary, our study is the first to identify and characterize the whole genome of pepper *CaRAVs*, including chromosome location, protein structure and domain, phylogenetic tree and collinearity information. We found that *CaRAVs* and *SIRAVs* are closely related to each other. Under low-temperature conditions, we determined the relative expression of *CaRAVs* using qRT-PCR and screened out three genes, *CaRAVI*, *CaRAV2*, and *CaNGAI*, which are relatively more sensitive to chilling stress, from which two genes with different structural domains (*CaRAVI* and *CaNGAI*) were selected for the construction of silencing vectors. The results showed that the silenced plants produce greater levels of REC and SOD when they are not stressed (Ctl). However, the *RAVI*-silenced plants and *NGAI*-silenced plants exhibited more severe damage after low-temperature stress than did the V2 plants, with the pTRV2:*RAVI* plants exhibiting significantly greater MDA and REC levels than the other two plants. In addition, the POD and CAT enzyme activities of the silenced plants were significantly lower than those of the control plants after being subjected to low temperature, and after 24 h of recovery, the CAT enzyme activities of the silenced plants did not increase in a similar manner to those of the V2 plants.

Meanwhile, the relative expression of *CaSOD*, *CaPOD*, and *CaCAT* could be significantly greater in V2 plants compared to *RAVI*-silenced plants and *NGAI*-silenced plants. Suggesting that *CaRAVI* and *CaNGAI* positively regulate the response of pepper plants to chilling stress. Therefore, under chilling stress, understanding the RAV transcription factor response, it is important for determining the role of *CaRAVs* in the chilling response of pepper plants.

## Supplementary Information

The online version contains supplementary material available at <https://doi.org/10.1186/s12864-024-10639-x>.

Supplementary Material 1.

Supplementary Material 2.

## Acknowledgements

We appreciate the financial support given by the projects. We thank the teacher and all schoolmates in our laboratory for providing useful discussions and technical assistance. We are grateful to the editor and reviewers for their help and comments on the manuscript.

## Authors' contributions

MKP: Writing-original draft, Methodology, Data curation. PY: Data curation, Formal analysis, Investigation. Jian Li and YZW: Investigation, Methodology. Juan Li: Investigation. HJX: Supervision, Funding acquisition. Jie Li: Supervision, Writing—review & editing. All authors read and approved the final manuscript.

## Funding

This work was supported by the Xinjiang Uyghur Autonomous Region Key Research and Development Plan Project (2022B02032), Yunnan Fundamental Research Projects (202401AT070059), Yunnan Young and Middle Aged Academic and Technical Leaders Reserve Talents (202205AC160056).

## Availability of data and materials

The entire *Capsicum annuum* genome sequence information was obtained from the Ensembl Genomes website. The plant materials "Shenghan 740" used in the experiment were supplied by the Vegetable Research Center, Beijing Academy of Agriculture and Forestry Sciences. The datasets supporting the conclusions of this manuscript are included in the manuscript and its Supplementary Files.

## Declarations

### Ethics approval and consent to participate

All plant materials used in the current study complied with the relevant institutional, national, and international guidelines and legislation. This manuscript does not contain any studies with human participants or animals performed by the authors. These methods were carried out in accordance with relevant guidelines and regulations.

### Consent for publication

Not applicable.

### Competing interests

The authors declare no competing interests.

### Author details

<sup>1</sup>College of Horticulture, Xinjiang Agriculture University, Urumqi 830052, China. <sup>2</sup>College of Biological and Agricultural Sciences, Honghe University, Mengzi, Yunnan 661100, China. <sup>3</sup>College of Horticulture, Gansu Agriculture University, Lanzhou 730070, China. <sup>4</sup>College of Horticulture and Forestry, Tarim University, Alar 843300, China.

Received: 10 May 2024 Accepted: 19 July 2024

Published online: 29 July 2024

## References

- Wang Y, Deng D, Zhang R, Wang S, Bian Y, Yin Z. Systematic analysis of plant-specific B3 domain-containing proteins based on the genome resources of 11 sequenced species. *Mol Biol Rep*. 2012;39(5):6267–82.
- Peng F, Weselake RJ. Genome-wide identification and analysis of the B3 superfamily of transcription factors in Brassicaceae and major crop plants. *Theor Appl Genet*. 2013;126(5):1305–19.
- Qu J, Wang B, Xu Z, Feng S, Tong Z, Chen T, et al. Genome-Wide Analysis of the Molecular Functions of B3 Superfamily in Oil Biosynthesis in Olive (*Olea europaea* L.). *Biomed Res Int*. 2023;2023:6051511.
- Swaminathan K, Peterson K, Jack TP. The plant B3 superfamily. *Trends Plant Sci*. 2008;13(12):647–55.
- Fu M, Kang HK, Son SH, Kim SK, Nam KH. A subset of Arabidopsis RAV transcription factors modulates drought and salt stress responses independent of ABA. *Plant Cell Physiol*. 2014;55(11):1892–904.
- Osnato M, Matias HL, Aguilar JAE, Kater MM, Pelaz S. Genes of the RAV Family Control Heading Date and Carpel Development in Rice. *Plant Physiol*. 2020;183(4):1663–80.
- Zhao L, Hao D, Chen L, Lu Q, Zhang Y, Li Y, et al. Roles for a soybean RAV-like orthologue in shoot regeneration and photoperiodicity inferred from transgenic plants. *J Exp Bot*. 2012;63(8):3257–70.
- Guo BJ, Wei Y, Xu RG, Lin S, Luan HY, Lv C, et al. Genome-Wide Analysis of APETALA2/Ethylene-Responsive Factor (AP2/ERF) Gene Family in Barley (*Hordeum vulgare* L.). *PLoS ONE*. 2016; 11(9): 0161322.
- Kabir N, Lin H, Kong X, Liu L, Qanmber G, Wang Y, et al. Identification, evolutionary analysis and functional diversification of RAV gene family in cotton (*G. hirsutum* L.). *Planta*. 2022; 255: 1–16.
- Li XJ, Li M, Zhou Y, Hu S, Hu R, Chen Y, et al. Overexpression of Cotton RAV1 Gene in Arabidopsis Confers Transgenic Plants High Salinity and Drought Sensitivity. *PLoS ONE*. 2015;10(2):0118056.
- Li J, Song C, Li H, Wang S, Hu L, Yin Y, et al. Comprehensive analysis of cucumber RAV family genes and functional characterization of CsRAV1 in salt and ABA tolerance in cucumber. *Front Plant Sci*. 2023;14:1115874.
- Chen C, Li Y, Zhang H, Ma Q, Wei Z, Chen J, et al. Genome-Wide Analysis of the RAV Transcription Factor Genes in Rice Reveals Their Response Patterns to Hormones and Virus Infection. *Viruses*. 2021;13(5):752.
- Yamasaki K, Kigawa T, Inoue M, Tateno M, Yamasaki T, Yabuki T, et al. Solution structure of the B3 DNA binding domain of the arabidopsis cold-responsive transcription factor RAV1. *Plant Cell*. 2004;16(12):3448–59.
- Zhang J, Liang L, Xie Y, Zhao Z, Su L, Tang Y, et al. Transcriptome and Metabolome Analyses Reveal Molecular Responses of Two Pepper (*Capsicum annuum* L.) Cultivars to Cold Stress. *Front Plant Sci*. 2022; 13: 819630.
- Linbo C, Yeyun L, Qin W, Yong LG, Chang JJ. Cloning and expression analysis of RAV gene related to cold stress from tea plant (*Camellia sinensis*). *Plant Physiol Commun*. 2010;46(4):354–8.
- Du C, Hu K, Xian S, Liu CQ, Fan J, Tu J, et al. Dynamic transcriptome analysis reveals AP2/ERF transcription factors responsible for cold stress in rapeseed (*Brassica napus* L.). *Mol Genet Genomics*. 2016;291(3):1053–67.
- Song X, Li N, Zhang Y, Liang Y, Zhou R, Yu T, et al. Transcriptomics and Genomics Analysis Uncover the Differentially Expressed Chlorophyll and Carotenoid-Related Genes in Celery. *Int J Mol Sci*. 2022;23(16):8986.
- Liu Z, Cai S, Zhang S, Xiao Y, Devahastin S, Guo C, et al. A systematic review on fermented chili pepper products: Sensorial quality, health benefits, fermentation microbiomes, and metabolic pathways. *Trends Food Sci Tech*. 2023;141:104189.
- Dasgan HY, Yilmaz MT, Dere S, Kiz B, Gruda NS. Bio-Fertilizers Reduced the Need for Mineral Fertilizers in Soilless-Grown Capia Pepper. *Horticulturae*. 2023;9(2):188.
- Luo Y, Chen S, Wang P, Peng D, Zhang X, Li H, et al. Genome-Wide Analysis of the RAV Gene Family in Wheat and Functional Identification of TaRAV1 in Salt Stress. *Int J Mol Sci*. 2022;23(16):8834.
- Sanatombi K. Antioxidant potential and factors influencing the content of antioxidant compounds of pepper: A review with current knowledge. *Compr Rev Food Sci F*. 2023;22(4):3011–52.
- Dhindsa RS, Plumb-Dhindsa PL, Thorpe TA. Leaf Senescence: Correlated with Increased Levels of Membrane Permeability and Lipid Peroxidation,

- and Decreased Levels of Superoxide Dismutase and Catalase. *J Exp Bot.* 1981;32(1):93–101.
23. Yang Q, Zhang Z, Rao J, Wang Y, Sun Z, Ma Q, et al. Low-temperature conditioning induces chilling tolerance in "Hayward" kiwifruit by enhancing antioxidant enzyme activity and regulating endogenous hormones levels. *J Sci Food Agr.* 2013;93(15):3691–9.
  24. Jebara SH, Jebara M, Limam F, Aouani ME. Changes in ascorbate peroxidase, catalase, guaiacol peroxidase and superoxide dismutase activities in common bean (*Phaseolus vulgaris*) nodules under salt stress. *J Plant Physiol.* 2005;162(8):929–36.
  25. Almeselmani M, Deshmukh PS, Sairam RK, Kushwaha SR, Singh TP. Protective role of antioxidant enzymes under high temperature stress. *Plant Sci.* 2006;171(3):382–8.
  26. Biasini M, Bienert S, Waterhouse AM, Arnold K, Studer G, Schmidt T, et al. SWISS-MODEL: modelling protein tertiary and quaternary structure using evolutionary information. *Nucleic Acids Res.* 2014;42(1):252–8.
  27. Tiamiyu QO, Adebayo S, Ibrahim N. Recent advances on postharvest technologies of bell pepper: a review. *Heliyon.* 2023;9:e15302.
  28. Wang X, Li N, Zan T, Xu K, Gao S, Yin Y, et al. Genome-wide analysis of the TIFY family and function of CaTIFY7 and CaTIFY10b under cold stress in pepper (*Capsicum annuum* L.). *Front. Plant Sci.* 2023;14:1308721.
  29. Feng K, Hou XL, Xing GM, Liu JX, Duan AQ, Xu ZS, et al. Advances in AP2/ERF super-family transcription factors in plant. *Crit Rev Biotechnol.* 2020;40(6):750–76.
  30. Huang YL, Zhang L, Zhang K, Chen S, Hu JB, Cheng F. The impact of tandem duplication on gene evolution in Solanaceae species. *J Integr Agr.* 2022;21(4):1004–14.
  31. Hanada K, Zou C, Lehti SMD, Shinozaki K, Shiu SH. Importance of Lineage-Specific Expansion of Plant Tandem Duplicates in the Adaptive Response to Environmental Stimuli. *Plant Physiol.* 2008;148(2):1003–993.
  32. Clark RM, Schweikert GB, Toomajian C, Ossowski S, Zeller G, Shinn P, et al. Common Sequence Polymorphisms Shaping Genetic Diversity in *Arabidopsis thaliana*. *Science.* 2007;317:338–42.
  33. Rackovsky S, Scheraga HA. The structure of protein dynamic space. *P Natl Acad Sci.* 2020;117(33):19938–42.
  34. Castillo DCI, Mekhedov SL, Hartl DL, Koonin EV, Kondrashov FA. Selection for short introns in highly expressed genes. *Nat Genet.* 2002;31(4):415–8.
  35. Liu H, Lyu H, Zhu K, Van de Peer Y, Cheng ZM. The emergence and evolution of intron-poor and intronless genes in intron-rich plant gene families. *Plant J.* 2020.
  36. Wang DQ, Yang Z, Wu MX, Wang W, Wang Y, Nie S. Enhanced brassinosteroid signaling via the overexpression of SIBR1 positively regulates the chilling stress tolerance of tomato. *Plant Sci.* 2022;320:111281.
  37. Wang M, Zhang S, Ding F. Melatonin Mitigates Chilling-Induced Oxidative Stress and Photosynthesis Inhibition in Tomato Plants. *Antioxidants-Basel.* 2020;9(3):218.
  38. Wang H, Liu Z, Luo S, Li J, Zhang J, Li L, et al. 5-Aminolevulinic acid and hydrogen sulphide alleviate chilling stress in pepper (*Capsicum annuum* L.) seedlings by enhancing chlorophyll synthesis pathway. *Plant Physiol Bioch.* 2021;167:567–576.
  39. Yao M-m, Ge W, Zhou Q, Zhou X, Luo ML, Zhao Y-b, et al. Exogenous glutathione alleviates chilling injury in postharvest bell pepper by modulating the ascorbate-glutathione (AsA-GSH) cycle. *Food Chem.* 2021;352:129458.
  40. Korkmaz AS, Deger O, Szafrńska K, Koklu S, Karaca A, Yakupoglu G, et al. Melatonin effects in enhancing chilling stress tolerance of pepper. *Sci Hortic-Amsterdam.* 2021;289:110434.
  41. Tang C, Xie J, Lv J, Li J, Zhang J, Wang C, et al. Alleviating damage of photosystem and oxidative stress from chilling stress with exogenous zeaxanthin in pepper (*Capsicum annuum* L.) seedlings. *Plant Physiol Bioch.* 2021;162:395–409.
  42. Nandagopal JGT, Shanmugam G. Screening and differential oxidative stress responses of hot pepper (*Capsicum annuum* L.) genotypes under cold stress. *S Afr J Bot.* 2022;151:591–599.
  43. Ramakrishnan M, Zhang ZJ, Mullasserri S, Kalendar R, Ahmad Z, Sharma A, et al. Epigenetic stress memory: A new approach to study cold and heat stress responses in plants. *Front Plant Sci.* 2022;13:1075279.
  44. Li C, Ji J, Wang G, Li Z, Wang Y, Fan Y. Over-Expression of LcPDS, LcZDS, and LcCRTISO. Genes From Wolfberry for Carotenoid Biosynthesis, Enhanced Carotenoid Accumulation, and Salt Tolerance in Tobacco. *Front Plant Sci.* 2020;11:119.
  45. Sohag AAM, Tahjib UAM, Afrin S, Khan MK, Hannan MA, Skalicky M, et al. Insights into nitric oxide-mediated water balance, antioxidant defence and mineral homeostasis in rice (*Oryza sativa* L.) under chilling stress. *Nitric oxide.* 2020;100:7–16.
  46. Zhou W, Leul M. Uniconazole-induced tolerance of rape plants to heat stress in relation to changes in hormonal levels, enzyme activities and lipid peroxidation. *Plant Growth Regul.* 1999;27:99–104.
  47. Ding YF, Wang XT, Wang F, Shao Y, Zhang AM, Chang W. The effects of chilling stress on antioxidant enzymes activities and proline, malondialdehyde, soluble sugar contents in three paphiopedilum species. *Russ J Plant Physiol.* 2023;70(4):61.
  48. Wang X, An Z, Liao JZ, Ran N, Zhu Y, Ren S, et al. The Role and Mechanism of Hydrogen-Rich Water in the *Cucumis sativus* Response to Chilling Stress. *Int J Mol Sci.* 2023;24(7):6702.
  49. Gu K, Hou S, Chen J, Guo J, Wang F, He C, et al. The physiological response of different tobacco varieties to chilling stress during the vigorous growing period. *Sci Rep-Uk.* 2021;11(1):22136.
  50. Nai G, Liang G, Ma W, Lu S, Li Y, Gou H, et al. Overexpression VaPYL9 improves cold tolerance in tomato by regulating key genes in hormone signaling and antioxidant enzyme. *Bmc Plant Biol.* 2022;22(1):344.

## Publisher's Note

Springer Nature remains neutral with regard to jurisdictional claims in published maps and institutional affiliations.